THE ASTROPHYSICAL JOURNAL, 197:31–38, 1975 April 1

INTERSTELLAR SCINTILLATION OF EXTRAGALACTIC RADIO SOURCES

J. J. CONDON
National Radio Astronomy Observatory,* Charlottesville, Virginia

AND

D. C. BACKER†
Goddard Space Flight Center, Greenbelt, Maryland
Received 1974 August 23; revised 1974 October 11

ABSTRACT

Observations of 12 compact extragalactic sources were made at 2695 and 8085 MHz in order to detect weak intensity fluctuations caused by interstellar scintillation. Pulsar data are used to estimate the parameters of the interstellar medium needed to interpret the measured upper limits in terms of source angular diameters which are much larger than the scintillation cutoff diameter. It is shown that the observed source rms brightness temperatures are less than 10^{15} K and 10^{14} K at 2695 and 8085 MHz, respectively, making self-absorbed proton-synchroton radiation and high-brightness coherent mechanisms unlikely. If the sources are composed of "point" components, each source can contain no fewer than 10^4 such components.

Subject headings: radio sources — synchrotron radiation — interstellar medium

I. INTRODUCTION

The solid angle Ω which a radio source subtends is a fundamental parameter in the description of the source. Combined with the source flux density, it yields the effective brightness temperature T_B, an intensive quantity which is often crucial to deciding the emission mechanism and the values of other intensive quantities such as energy per particle or magnetic field strength. The sizes of extremely compact extragalactic radio sources are of particular interest because a variety of indirect measurements indicate that they have brightness temperatures close to or perhaps even exceeding the maximum theoretically obtainable in a stationary incoherent electron-synchrotron source, about 10^{12} K.

The most nearly direct method by which temperatures of compact sources have been obtained is very-long-baseline interferometry (VLBI). Interferometers with baselines limited to the Earth's diameter cannot resolve sources significantly brighter than 10^{12} K regardless of wavelength, however (Kellermann *et al.* 1971); and practical limitations of antenna siting and tracking have severely limited the baseline coverage of such measurements. There are several sources whose angular dimensions in one coordinate have been estimated as $\theta \sim 10^{-3}$ arcsec in this way; but these angles may just represent the maximum spacing between two or more very compact components, rather than the diameters of single sources. Thus current very-long-baseline observations show that very compact sources exist, but can only set upper limits $\Omega \leqslant \theta^2$ to the solid angles which they subtend.

Brightness temperatures greater than 10^{12} K might be produced during brief outbursts in an incoherent electron-synchrotron source. Alternatively, the maximum brightness temperature of an incoherent proton-synchrotron source is a factor $(m_p/m_e)^{3/2} = 8 \times 10^4$ higher, and the limits for a number of coherent emission mechanisms are higher yet. The only observational evidence for the possible existence of such very compact components in extragalactic radio sources are rapid intensity variations which are presumed to arise from emitting regions smaller than the variation time scale multiplied by the speed of light. Although the light travel time argument breaks down when relativistic source expansion is considered (Rees 1967), the recently observed low-frequency variability of 3C 454.3 (Hunstead 1972) is still difficult to interpret in terms of conventional incoherent electron-synchrotron components, particularly if the quasar redshifts are cosmological (Jones and Burbidge 1973).

Resolutions exceeding those of Earth-based interferometery are required to measure brightness temperatures exceeding 10^{12} K. In this paper we show that the method of measuring the extragalactic source intensity fluctuations due to interstellar scintillation suggested by Lovelace and Backer (1972) is an effective and direct way to obtain source solid angles in the range $\Omega = 10^{-5}$ to 10^{-1} (milli-arcsec)^2. The observations of known compact extragalactic sources for the purpose of obtaining their scintillation indices are described in § II. The "calibration" of the interstellar medium point-source response from pulsar data is explained in § III. The relation between scintillation index and source effective solid angle is derived for the case in which the source diameter is much greater than the scintillation cutoff diameter. Finally, in § IV the implications of these measurements in terms of emission mechanisms of very compact extragalactic sources are discussed.

* Operated by Associated Universities, Inc., under contract with the National Science Foundation.

† NAS/NRC Resident Research Associate.

II. INTENSITY FLUCTUATION MEASUREMENTS

Sources which were known to contain a significant fraction of their flux density in a small angular size were observed, subject to the observational constraints of limited sensitivity and integration time. The most direct measurements of compact source angular diameters come from very-long-baseline interferometry. Published diameters are resolution-limited at about 0".001, and the baseline coverage is extremely limited. We have computed the one-dimensional equivalent Gaussian diameter θ_g between half-intensity points from published fringe visibilities measured near interferometer transit on 10^8 λ baselines at 13 cm (Kellermann *et al.* 1970) and 3.8 cm (Cohen *et al.* 1971). Upper limits to unresolved source diameters were calculated taking 20 percent and 10 percent overall fringe amplitude calibration uncertainties at 13 and 3.8 cm, respectively, into account. The θ_g for the compact sources that we selected to observe are listed in table 1. We note that they may be used to estimate lower limits for the scintillation indices expected from these sources because almost any other structures yielding the same measured fringe visibilities would produce stronger scintillation. Also it appears to be conservative to use the 13-cm data to estimate 11-cm source diameters, since a comparison of 18-cm and 6-cm fringe visibilities of compact sources uncovered no source whose diameter decreases with increasing wavelength (Kellermann *et al.* 1971).

Spectral evidence of synchrotron self-absorption also suggests that most of the sources in table 1 subtend very small solid angles (Kellermann and Pauliny-Toth 1969). Equivalent circular Gaussian diameters as small as 0".0002 for 4C 38.41 at 3.8 cm are plausible (Pauliny-Toth *et al.* 1973), but they may increase so rapidly with wavelength (Condon and Dressel 1973) that the 13-cm diameter limits cannot be reduced with confidence.

Rapid intensity variations of the BL Lacertae objects VRO 42.22.01 (MacLeod *et al.* 1971) and OJ 287 (Andrew, Harvey, and Medd 1971) and the QSO PKS 0106+01 (Wills 1971), as well as the surprising low frequency variability of CTA 102 and 3C 454.3 (Hunstead 1972), may indicate the presence of very compact components. If components varying on a time scale τ have linear dimensions less than $c\tau$, the angular diameters deduced are distance dependent, and may not be so very small if the QSO redshifts are noncosmological (Jones and Burbidge 1973). Finally, the sources 3C 120 and 3C 279 were included because of their apparently supraluminal structural variability.

TABLE 1

VLBI EQUIVALENT GAUSSIAN DIAMETERS OF THE COMPACT SOURCES OBSERVED

Source	Type	Equivalent Diameters θ_g (milli-arcsec) at	
		13 cm	3.8 cm
PKS 0106+01	QSO	< 1.0	< 0.7
3C 84	GAL	⩾2*	1.3
3C 120	GAL	1.8	2.0
OJ 287	LAC	...	< 0.4
3C 279	QSO	1.6	1.5
DW 1555+00	QSO	< 0.9	< 0.9
CTD 93	EF	1.9	...
4C 38.41	...	1.4*	...
PKS 2145+06	QSO	0.9	< 1.0
VRO 42.22.01	LAC	1.7	0.6
CTA 102	QSO	1.8	...
3C 454.3	QSO	1.3	0.9

*Pauliny-Toth, private communication.

Thus table 1 lists sources which are all known to be compact from VLBI observations. Sources showing evidence of sub-milli-arcsec structure by having high-frequency spectral peaks, rapid intensity variability, or unusual structure variability have also been included. All three basic classes of extragalactic radio sources (QSO, galaxy, and BL Lacertae object), as well as one empty field (EF), are represented. If very compact components are at all common in any type of extragalactic source, they should appear in one or more of the sources in our observing list.

The NRAO three-element interferometer was used to measure fluctuations in the 11-cm (2695 MHz) and 3.7-cm (8085 MHz) flux densities of the compact sources in table 1 and the four calibrators 3C 48, 3C 138, 3C 286, and 3C 395. Simultaneous dual-frequency observation permits some distinction to be made between scintillations and intrinsic variability, since intrinsic variations would be more strongly correlated than scintillation over such a wide frequency range. All of the sources are completely unresolved by the interferometer on the three baselines used (100, 1800, and 1900 m). The triply redundant amplitude information available at each frequency made it easy to detect and reject bad scans which might have passed unnoticed in single-antenna observations.

The observations and data reduction methods were designed for maximum sensitivity to small intensity fluctuations occurring on time scales longer than the 1-hour characteristic short-wavelength scintillation time scale of nearby pulsars. External accuracy and even accuracy in the relative flux densities of the different sources were sacrificed to maximize internal consistency. Receiver noise is quite small on the strong sources chosen after only 5 minutes of integration, so the largest sources of error are intensity proportional and tend to be systematically dependent on source declination and hour angle. Declination dependence is irrelevant to our measurements; but the hour angle dependence is not, as each source was observed over a wide range of hour angles on each day. Systematic pointing errors in each antenna, small mismatches in the interferometer delay elements, and atmospheric extinction are possible causes of such repeatable intensity-proportional errors. Regardless of their origin, they may be largely removed by scheduling observations on a strict 24 sidereal hour cycle and comparing observations of a source made at any particular hour angle on different days. Each source was therefore tracked for 5 minutes at intervals of precisely 1 hour for the 10 hours that it was visible each day. The day-to-day scan timing differences were less than 5 seconds. Four consecutive days of observations were made to provide enough independent data to determine the systematic errors and to detect intensity fluctuations with time scales less than 100 hours.

The method by which systematic intensity-proportional errors were removed is best explained by an example. The compact QSO PKS 0106+01 was observed daily at the ten hour angles shown in figure 1*a*. The ordinate is the uncorrected 2695 MHz "count," which is proportional to fringe amplitude, for the 1900-m baseline. The uncorrected counts are divided by the 2695-MHz time-dependent gain shown in figure 2, which is determined from the calibration sources as described below. This operation, which corresponds to the usual calibration of relative flux density measurements, results in the calibrated counts of figure 1*b*.

There is a separate hour-angle–dependent gain curve *G*(HA) for each source and baseline, determined by making a logarithmic least-squares fit to all the calibrated counts treated as functions of hour angle alone. For each day's data, a free adjusting constant was temporarily added to the logarithms of the counts so that long-term variations and missing data at some hour angles would not affect the fit. This adjusting constant was determined iteratively so that the harmonic mean of the adjusted counts over the hour angles available was the same on each day. Thus the data in figure 1*b* were used to compute the hour-angle–dependent gain curve of figure 1*c*. Because *G*(HA) is determined from averages over several days, it responds only weakly to the calibration source observations, whose main use is the determination of the slowly varying time-dependent gain curves. Their principal value is rather to allow more sensitive detection of scintillations occuring on short (1–10 hours) time scales. Since the hour-angle–dependent gain curves are applied equally to each day's data, they do not affect the measured day-to-day fluctuations listed in table 2. The corrected counts shown in figure 1*d* are the calibrated counts of figure 1*b* divided by the hour-angle–dependent gain curve.

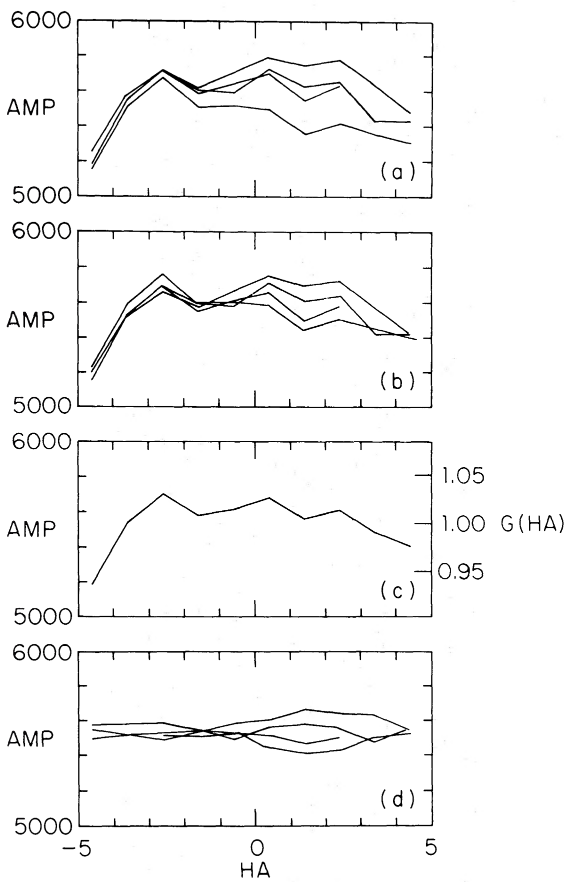

FIG. 1.—Stages in the reduction of 1900-m baseline, 2695 MHz fringe amplitudes for PKS 0106+01. The uncorrected values (*a*) are calibrated (*b*) and divided by the hour-angle–dependent gain (*c*) to yield the final corrected amplitudes (*d*).

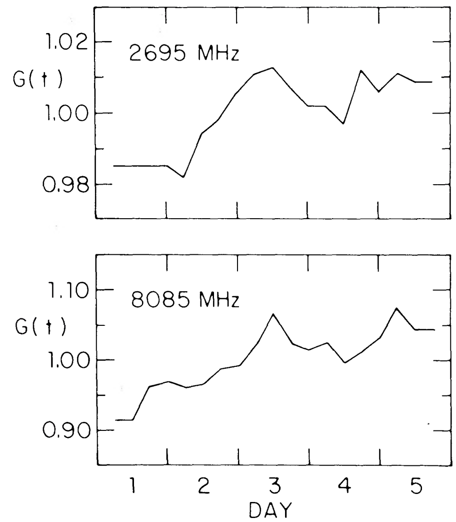

FIG. 2.—Time dependence of interferometer gain

Similar corrected counts were computed for all sources and baselines at both 2695 and 8085 MHz. The rms scatter in the corrected count at these two frequencies is typically less than 1 percent and 2 percent, respectively. No significant variations on 1-hour time scales were detected at this level in any source at either frequency. The corrected counts were then averaged over hour angles and baselines to give the mean daily amplitude of each source at each frequency. These mean amplitudes were normalized to unity and plotted in figure 3 to show the day-to-day fractional intensity fluctuations, whose rms values are listed in table 2. Again, no significant variations were detected. Thus the fluctuations listed in table 2, which are due to receiver noise, calibration errors, intrinsic source variations, and scintillations in unknown proportion, are taken to be upper limits to any scintillations that may exist. These upper limits are used in § III to set constraints on the angular structures of the sources observed.

The time-dependent gain correction factors of

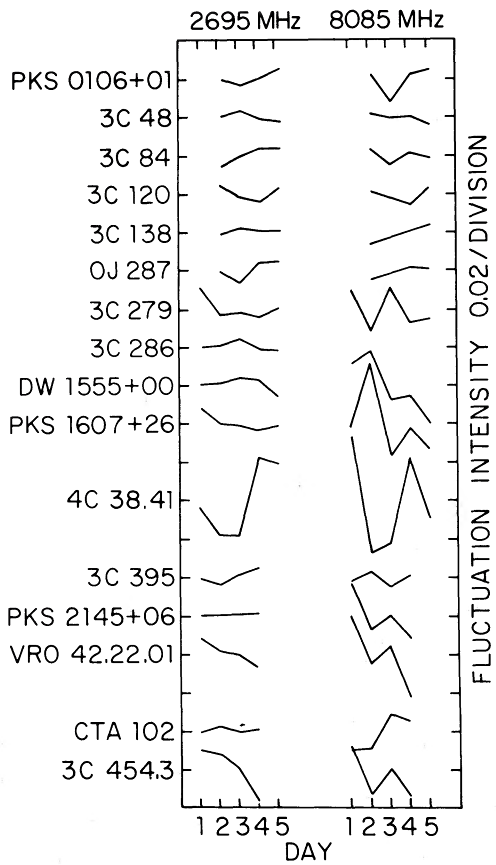

FIG. 3.—Observed fluctuations in the daily averages of source intensity at 2695 and 8085 MHz.

figure 2 were themselves determined iteratively by requiring that they minimize the day-to-day amplitude fluctuations observed on the calibration sources 3C 48, 3C 138, 3C 286, and 3C 395. A further requirement that the harmonic mean of the points contributed by each calibration source to the time-dependent gain curves be unity ensures that errors in the assumed relative flux densities of the calibrators do not cause apparent intensity fluctuations in the compact sources. The calibration sources were selected for being small enough that they are unresolved by the NRAO interferometer, but large enough that they are unlikely to exhibit scintillations or intrinsic variations. Both 3C 48 and 3C 286 are completely resolved at 13 cm on $80 \times 10^6\,\lambda$ baselines (Kellermann *et al.* 1970), and 3C 138 and 3C 395 appear to be nonvariable and have the steep spectra characteristic of extended, optically thin sources.

TABLE 2

DAY-TO-DAY RMS INTENSITY FLUCTUATIONS

Source	RMS Fluctuations (percent) at 11 cm	3.7 cm
PKS 0106+01..........	0.4	0.8
3C 48..................	0.2	0.2
3C 84..................	0.5	0.3
3C 120.................	0.4	0.5
3C 138.................	0.1	0.5
OJ 287.................	0.5	0.3
3C 279.................	0.6	1.0
3C 286.................	0.2	0.6
DW 1555+00..........	0.4	1.5
CTD 93................	0.4	1.9
4C 38.41...............	1.9	2.7
3C 395.................	0.4	0.4
PKS 2145+06..........	0.1	1.3
VRO 42.22.01..........	0.6	1.8
CTA 102...............	0.1	1.0
3C 454.3...............	1.2	1.4

III. SCINTILLATION CALIBRATION

Converting the measured scintillation index μ of an extended extragalactic source, which is the rms fractional deviation of the signal from its mean, to the effective solid angle Ω_e of the source requires calibration of the interstellar medium point-source response on the basis of pulsar scintillation studies. The five parameters needed are the radio frequency ν_c, which divides the weak and strong scattering regimes, as a function of dispersion measure DM; the diffraction pattern scale size a and bandwidth f_0 of the scintillation spectrum as a function of DM and radio frequency ν; the maximum dispersion measure as a function of galactic latitude b; and the effective height z_s of the scattering screen above the galactic plane.

Observations at centimeter wavelengths (Downs and Reichley 1971; Backer and Fisher 1974; Backer 1975) are consistent with

$$\nu_c = 0.5\,\mathrm{DM}\,(\mathrm{GHz})\,, \qquad (1)$$

where all radio frequencies are expressed in GHz and dispersion measures in parsec cm^{-3} in this and subsequent equations. The scintillation fluctuation spectrum $P_0(f)$ of a point source of unit intensity deduced from pulsar measurements (Rickett 1970; Lang 1971; Boriakoff 1973; Backer 1975) is the Gaussian

$$P_0(f) = \frac{(2/\pi f_0)^{1/2}}{1 + (\nu/\nu_c)^2} \exp\left(-f^2/2f_0^2\right)\,, \qquad (2)$$

where

$$f_0 = 4 \times 10^{-5}(1 + \nu/\nu_c)\,\mathrm{DM}\,\nu^{-1}\,(\mathrm{Hz})\,.$$

Multiple station observations of the instantaneous decorrelation of pulsar scintillation at 327 and 408 MHz (Slee *et al.* 1974; Backer, Lyne, and Zeissig 1974, respectively) yield a value for the diffraction pattern scale size of

$$a = 1.4 \times 10^{10}\left(1 + \frac{\nu}{\nu_c}\right)^{-1} \mathrm{DM}^{-1/2}\,\nu\,(\mathrm{cm})\,. \qquad (3)$$

The upper envelope of pulsar dispersion measures shown in figure 4, which is

$$\mathrm{DM} = 25 \csc|b|\,(\mathrm{pc\ cm^{-3}})\,, \qquad (4)$$

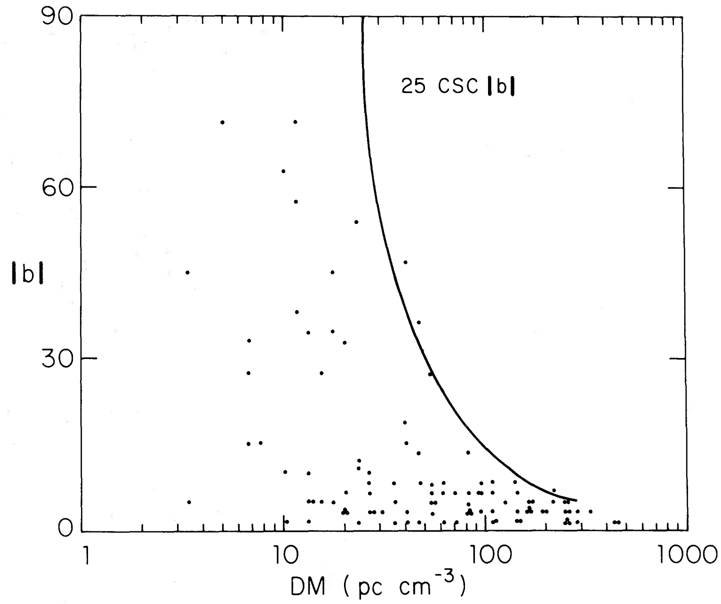

FIG. 4.—Pulsar dispersion measures at different absolute values of galactic latitude. The upper envelope, approximated by 25 csc $|b|$, is used to calculate the extragalactic source dispersion measures.

gives the extragalactic source dispersion measures for a plane-parallel approximation to the galactic electron disk. If the electron density decreases linearly with z from its local value of 0.04 cm^{-3} (Gordon and Gordon 1973), it falls to zero at a "half-thickness" $z = 600$ pc. Lyne (1973) suggests a half-thickness of 230 pc based on a pulsar search complete for $|b| \leq 10°$, and Falgarone and Lequeux (1973) find values near 350 pc, assuming the above local electron density. We place the theoretical thin scattering screen at half the first value, which is consistent with pulsar dispersion measures, (eq. [4]), or

$$z_s = 300 \csc |b| \text{ (pc)} . \quad (5)$$

It should be noted that, for extended source observations in the regime of strong scattering, an observer well beyond the focal length of the majority of the density irregularities in a distributed scattering medium may want to consider only that closest portion of the medium which just produces strong scattering at the observing radio frequency, rather than the entire medium. This would be particularly relevant to observations at lower radio frequencies. A more detailed discussion of the origins and relations of the above scintillation parameters is given by Backer (1975).

We note that the effective pattern speed $u \equiv a/\tau$, where $\tau \equiv (2^{1/2}\pi f_0)^{-1}$, is 50 km s^{-1} from equations (2) and (3) with DM = 16. It is comparable to the magnitude of the projection u_c on the celestial sphere of the vector sum of velocity components due to the Earth's orbital motion, solar velocity relative to the local standard of rest, and differential galactic rotation

TABLE 3

PREDICTED INTERSTELLAR SCINTILLATION PARAMETERS

Source	b (deg)	2.7 GHz (percent) μ_1	2.7 GHz (percent) μ_2	8.1 GHz (percent) μ_1	8.1 GHz (percent) μ_2	u_c (km s^{-1})
PKS 0106+01	−61	>0.2	>0.1	0.6	0.3	14
3C 84............	−13	0	0	0.1	0	34
3C 120...........	−27	0	0	0.2	0	23
OJ 287...........	36	0.1	0	0.7	0.4	29
OK 290..........	51	(0.2)	(0.1)	(0.4)	(0.1)	25
3C 279...........	57	0.1	0	0.3	0.1	17
DW 1555+00	37	>0.1	>0.1	>0.3	>0.1	19
CTD 93..........	46	(0.2)	(0.1)	(0.3)	(0.1)	16
4C 38.41.........	42	0.1	0	(0.3)	(0.1)	21
PKS 2145+06	−34	0.1	0.1	>0.3	>0.1	25
BL Lac..........	−11	0	0	0.1	0	30
CTA 102.........	−39	0.1	0	(0.3)	0.1	24
3C 454.3.........	−38	0.1	0	0.3	0.1	24

of the screen. The u_c are listed in table 3 for the directions to the extragalactic sources observed. Possible calibration bias due to large pulsar proper motions (Gunn and Ostriker 1970; Manchester, Taylor, and Van 1974) is therefore small.

The effective angular diameter of structure in the scintillation diffraction pattern is $\psi = a/z_s$, or

$$\psi = 0.7 \times 10^{-3}\left(1 + \frac{\nu}{\nu_c}\right)^{-1} \nu \sin^{3/2}|b| \,, \qquad (6)$$

where ψ is in milli-arcsec. This revises downward the number given by Lovelace and Backer (1972) for two reasons: a, which is the product of u and τ, is a factor of 2.2 smaller based on more recent measurements and a different definition of the quantity; and z_s is 6 times larger, based on a more representative model of the interstellar plasma. We note that if equation (4) overestimates the plasma column density at high galactic latitudes, ψ would increase, and the expected scintillation index of an extended source would increase, unless the scattering became weak. Also, if only a nearby portion of the medium is effective as mentioned above, ψ and the scintillation index would both increase. The directional inhomogeneities of scattering observed by Readhead and Hewish (1972) and Backer (1974) also emphasize that our results are statistical in nature.

The scintillation index of an extragalactic point source is obtained from the fluctuation spectrum:

$$\mu_0 = \left[\int_{-\infty}^{\infty} P_0(f)df\right]^{1/2} . \qquad (7)$$

If the source is extended, the diffraction pattern is convolved with the source brightness distribution. This convolution corresponds to multiplication of $P_0(f)$ in equation (7) by $V(z_s f/u)$, the integral along the axis perpendicular to the direction of u of the absolute square of the two-dimensional source visibility function. The filtered spectrum $P_1(f)$ is integrated as in equation (7) to produce the extended source scintillation index μ_1. For example, the scintillation spectrum of a circular Gaussian source of diameter θ between half-intensity points is (Cohen, Gundermann, and Harris 1967)

$$P_1(f) = \left(\frac{2}{\pi f_1^2}\right)^{1/2}\left(\frac{f_1}{f_0}\right)\left[1 + \left(\frac{\nu}{\nu_c}\right)^2\right]^{-1} \exp\left(\frac{-f^2}{2f_1^2}\right) , \qquad (8)$$

where

$$f_1 = f_0[1 + 0.36(\theta/\psi)^2]^{-1/2} .$$

The asymptotic forms of $P_1(f)$ and μ_1 in the limit that the source angular size is much greater than ψ are important for interstellar scintillation studies of extragalactic sources because $\psi \approx 10^{-3}$ milli-arcsec. If a source is "everywhere extended" in the sense that it has no structure smaller than ψ, then the source visibility function is small at frequencies above f_0 and the approximation $P_0(f) \approx$ constant may be made in equation (7). The scintillation index μ_1 is proportional to $(\int |V|^2 df)^{1/2}$. If the effective solid angle Ω_e subtended by a source with brightness distribution $B(\alpha, \delta)$ is defined to be

$$\Omega_e \equiv \frac{[\int B(\alpha, \delta)d\alpha d\delta]^2}{\int B^2(\alpha, \delta)d\alpha d\delta} , \qquad (9)$$

then application of Rayleigh's theorem (Bracewell 1965) in two dimensions shows that the scintillation index μ_1 is proportional to $\Omega_e^{-1/2}$ for all everywhere extended brightness distributions. The scintillation index is, in other words, proportional to the rms brightness temperature of the source.

A low value of μ_1 is not sufficient to prove that a source is everywhere extended, even for known strong scattering. A compact extragalactic source might be comprised of a large number of point sources distributed over an area 1 milli-arcsec in diameter, for example. In such a case, the visibility function of each point source can be treated as independent of fluctuation frequency during the calculation of μ_1. A lower limit to the number N of point sources can be obtained by supposing that their angular spacing is greater than ψ. The sources then scintillate independently, and we have the limit

$$N > \mu_1^{-2} . \qquad (10)$$

Observations of intensity fluctuations about the mean taken over a finite interval T act as a high-pass filter on the observed extended source scintillation spectra. This observing filter frequency response is approximately

$$O(f) = 1 - \sin^2(\pi f T)/(\pi f T)^2 . \qquad (11)$$

Defining $P_2(f) \equiv O(f)P_1(f)$ allows the expected scintillation index μ_2 to be calculated as in equation (7).

An example of the source size and observing period filtering effects discussed above is given in figure 5. The three scintillation spectra of an imaginary circular Gaussian source of diameter $\theta = 10^{-5}$ arcsec at $|b| = 50°$ observed for 4 days at 8.1 GHz are shown. The scintillation index is $\mu_2 = 0.56$. In figure 6 the spectra are plotted for similar observations of PKS 0106+01 with θ equal to the equivalent diameter given in table 1. Note the changes in both scales. In this case $\mu_2 = 0.003$ for $T = 4$ days, a value just below the limits of our observations. Extending the observations over 2 weeks or more would bring μ_2 nearer to $\mu_1 = 0.006$. On these longer time scales, however, the intrinsic variations mentioned in § II can become important: μ_1 increases with radio frequency up to $\nu = \nu_c$, so that scintillations can mimic intrinsic variability. The two might be distinguishable through the limited correlation bandwidth of strong scattering scintillations or the power-law low-frequency (inverse months) fluctuation spectrum of intrinsic variations.

Table 3 gives the values of μ_1 and μ_2 calculated on the assumption that the sources are circular Gaussians whose diameters equal the sizes in table 1. Estimates enclosed in parentheses are calculated from $\theta = 1$ milli-arcsec. The variation of μ_1 with radio frequency

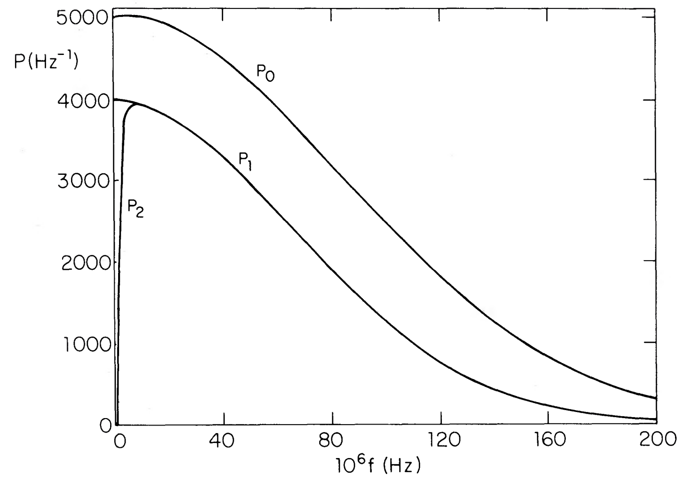

FIG. 5.—Predicted scintillation spectra of sources at $|b| = 50°$ observed at 8085 MHz. The spectra of a point source (P_0), a circular Gaussian source of 10^{-5} arcsec diameter (P_1), and the spectrum $P_1(f)$ after removal of a 4-day-long running mean (P_2) are plotted.

ν for a point source, and with source angular diameter θ for an extended source observed at $\nu = 8.1$ GHz are plotted in figure 7. We see that most of the sources in table 3 must subtend solid angles $\Omega_e > 0.003\ \theta_g^2$ at 2.7 GHz or $\Omega_e > 0.01\ \theta_g^2$ at 8.1 GHz.

IV. SOURCE MODELS

The very low upper limits to μ_2 which are listed in table 2 eliminate the possibility that compact extragalactic radio source emission comes primarily from a few powerful sources having angular diameters less than 10^{-2} or 10^{-3} milli-arcsec. If point sources do produce the radio radiation, at least 10^4 per source are required.

If extragalactic sources do not have significant structure on angular scales of 10^{-2} or 10^{-3} milli-arcsec, then upper limits to their brightness temperatures may be set from their flux densities and scintillation effective solid angle limits. For most of the compact sources in table 3 the maximum rms brightness temperatures are 10^{15} K at 2.7 GHz and 10^{14} K at 8.1 GHz. These values are only two orders of magnitude above the maximum permitted by inverse Compton cooling in incoherent electron-synchrotron sources. They discourage the application of models which require the higher brightness temperatures attainable with coherent emission to explain rapid intensity variability of extragalactic sources, at least at centimeter wavelengths. The scintillation observations are not inconsistent with coherent emission in 3C 454.3 producing the observed meter-wavelength variability, so long as the coherent emission is confined to decimeter wavelengths.

The scintillation lower limits to Ω_e can also be used to reject self-absorbed proton-synchrotron radiation as a means of obtaining rapid variability and high brightness temperatures. Self-absorption is required

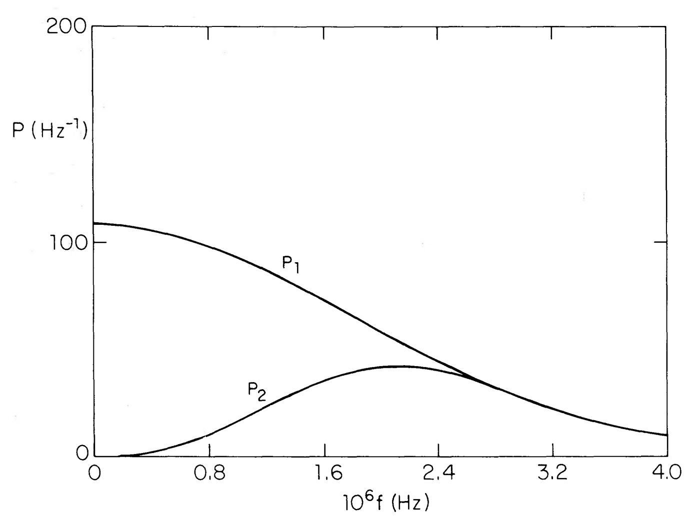

FIG. 6.—Predicted 8085 MHz scintillation spectrum (P_1) for a 7×10^{-4} arcsec diameter circular Gaussian model of the source PKS 0106+01. P_2 is the spectrum that would be observed by observations 4 days in length.

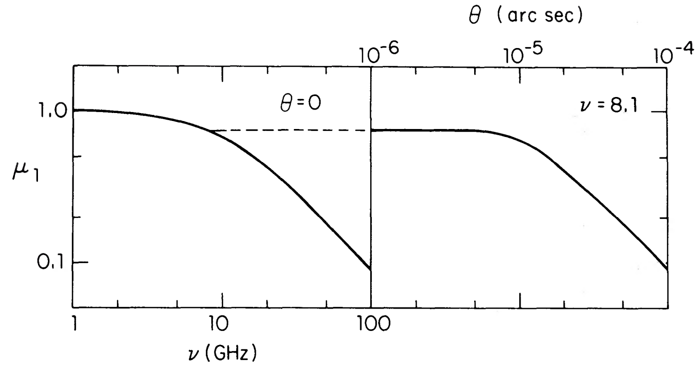

FIG. 7.—The variation of scintillation index μ_1 with radio frequency for a point source is shown in the left part of the figure. At a particular frequency, 8.1 GHz, the decrease of μ_1 with source diameter θ from its maximum point-source value is shown on the right.

to explain the spectra of most of the compact sources observed. The brightness S/Ω and magnetic field strength H of an optically thick proton-synchrotron source are related by

$$\frac{S}{\Omega} = 0.021 \left(\frac{m_p}{m_e}\right)^{3/2} \frac{\nu^{5/2}}{(1+z)^{1/2} H_\perp{}^{1/2}}, \qquad (12)$$

with the following units:

$$S\,(\mathrm{Jy}), \quad \Omega\,(\text{milli-arcsec})^2,$$
$$\nu\,(\mathrm{GHz}), \quad H_\perp\,(\mathrm{gauss}).$$

Once the source spectrum $S(\nu)$ and solid angle Ω are known, $H_\perp$ is determined. The magnetic energy density is then proportional to $(m_p/m_e)^6 = 4 \times 10^{19}$. Reasonable values of the total magnetic energy are possible only for very small values of Ω for proton-synchrotron sources which are self-absorbed above $\nu \approx 5$ GHz. When the observed lower limits to Ω_e are inserted into equation (12), the total magnetic energy requirements are seen to exceed 10^{61} ergs for most of the sources in table 3.

REFERENCES

Andrew, B. H., Harvey, G. A., and Medd, W. J. 1971, *Ap. Letters*, **9**, 151.
Backer, D. C. 1974, *Ap. J.*, **190**, 667.
———. 1975, in preparation.
Backer, D. C., and Fisher, R. F. 1974, *Ap. J.*, **189**, 137.
Backer, D. C., Lyne, A. G., and Zeissig, G. A. 1974, One Day Meeting on Interstellar Scattering of Radio Waves, Pasadena, California.
Boriakoff, V. 1973, Ph.D. thesis, Cornell University.
Bracewell, R. N. 1965, *The Fourier Transform and Its Applications* (New York: McGraw-Hill).
Cohen, M. H., Cannon, W., Purcell, G. H., Shaffer, D. B., Broderick, J. J., Kellermann, K. I., and Jauncey, D. L. 1971, *Ap. J.*, **170**, 207.
Cohen, M. H., Gundermann, E. J., and Harris, D. E. 1967, *Ap. J.*, **150**, 767.
Condon, J. J., and Dressel, L. L. 1973, *Ap. Letters*, **15**, 203.
Downs, G. S., and Reichley, P. E. 1971, *Ap. J.* (*Letters*), **163**, L11.
Falgarone, E., and Lequeux, J. 1973, *Astr. and Ap.*, **25**, 253.
Gordon, K. J., and Gordon, C. P. 1973, *Astr. and Ap.*, **27**, 119.
Gunn, J. E., and Ostriker, J. P. 1970, *Ap. J.*, **160**, 979.
Hunstead, R. W. 1972, *Ap. Letters*, **12**, 193.
Jones, T. W., and Burbidge, G. R. 1973, *Ap. J.*, **186**, 791.
Kellermann, K. I., Clark, B. G., Jauncey, D. L., Cohen, M. H., Shaffer, D. B., Moffet, A. T., and Gulkis, S. 1970, *Ap. J.*, **161**, 803.
Kellermann, I. I., Jauncey, D. L., Cohen, M. H., Shaffer, D. B., Clark, B. G., Broderick, J., Rönnäng, B., Rydbeck, O. E. H., Matveyenko, L., Moiseyev, I., Vitkevitch, V. V., Cooper, B. F. C., and Batchelor, R. 1971, *Ap. J.*, **169**, 1.
Kellermann, K. I., and Pauliny-Toth, I. I. K. 1969, *Ap. J.* (*Letters*), **155**, L71.
Lang, K. R. 1971, *Ap. J.*, **164**, 249.
Lovelace, R. V. E., and Backer, D. C. 1972, *Ap. Letters*, **11**, 135.
Lyne, A. G. 1973, IAU Session on Interstellar Medium, Sydney, Australia.
MacLeod, J. M., Andrew, B. H., Medd, W. J., and Olsen, E. T. 1971, *Ap. Letters*, **9**, 19.
Manchester, R. N., Taylor, H. H., and Van, Y. Y. 1974, *Ap. J.* (*Letters*), **189**, L119.
Pauliny-Toth, I. I. K., Preuss, E., Witzel, A., Kellermann, K. I., Fomalont, E. B., and Davis, M. M. 1973, *Astr. and Ap.*, **27**, 475.
Readhead, A. C. S., and Hewish, A. 1972, *Nature*, **236**, 440.
Rees, M. J. 1967, *M.N.R.A.S.*, **135**, 345.
Rickett, B. J. 1970, *M.N.R.A.S.*, **150**, 67.
Slee, O. B., Ables, J. G., Batchelor, R. A., Krishna-Mohan, S., Venugopal, V. R., and Swarup, G. 1974, *M.N.R.A.S.*, **167**, 31.
Wills, B. J. 1971, *Ap. J.*, **169**, 221.

D. C. BACKER: Goddard Space Flight Center, Code 693, Greenbelt, MD 20770

J. J. CONDON: Department of Physics, Virginia Polytechnic Institute and State University, Blacksburg, VA 24061